Preparation, Structure, and Magnetic Properties of a Ternary Tetrathiafulvalenium Salt Based on a Paramagnetic Hexanuclear Niobium Cluster Halide: $(TTF^+)_2[(Nb_6Cl_{18})^{3-}][(C_2H_5)_4N^+][CH_3CN]$, a Unique Molecular Rock Salt with Channels Incorporating a Neutral Organic Molecule

Alain Pénicaud, Patrick Batail,* Patrick Davidson, and Anne-Marie Levelut

Laboratoire de Physique des Solides Associé au CNRS, Université de Paris-Sud, 91405 Orsay, France

Claude Coulon

Centre de Recherche Paul Pascal, CNRS, Domaine Universitaire de Bordeaux I, 33405 Talence, France

Christiane Perrin

Laboratoire de Chimie Minérale B Associé au CNRS, Université de Rennes I, 35042 Rennes, France

Received July 31, 1989

A ternary tetrathiafulvalenium (TTF^+) salt, based on the trivalent, paramagnetic, hexanuclear, all-inorganic niobium cluster anion $Nb_6Cl_{18}^{3-}$, has been prepared by electrocrystallization and characterized by single-crystal X-ray diffraction and diffuse scattering as well as variable-temperature ESR studies. $(TTF^+)_2[(Nb_6Cl_{18})^{3-}][(C_2H_5)_4N^+][CH_3CN]$ is insulating, and the tetragonal (space group $P4_2/ncm$) lattice parameters at 140 K are a = 17.929 (6), c = 15.798 (3) Å, and V = 5079.0 Å^3. The structure presents a rock salt framework with the tetrahedral interstices selectively occupied by tetraethylammonium cations and acetonitrile molecules. The triplet state of the organic dimer is partially populated at high temperature and interacts with the localized niobium cluster spins. The latter do not interact directly with each other. The calculated magnetic gap of 0.07 eV for the dimer agrees with the experimental value of 0.07–0.10 eV deduced from an analysis of the spin susceptibility.

Introduction

Anticipating the site preference of a molecule or a molecular ion in crystalline solids is not usually possible. Indeed, the structural chemistry methodology[1] which has proven so successful in the description and prediction of the crystal structures of simple inorganic salts has no equivalent in molecular solid-state chemistry yet. Nevertheless, the rational geometrical description of extended molecular arrays, be they organic or inorganic in nature, is the focus of increasing attention.[2] To develop such a solid-state chemistry of molecular ions, we have set out to explore the solid-state associations between tetrathiafulvalene (TTF)-based cation radicals and the large all-inorganic hexanuclear molecular cluster halides $Mo_6Cl_{14}^{2-}$,[3] $Re_6Se_5Cl_9^-$,[4] and $Nb_6Cl_{18}^{3-}$.[5] In this paper, we report the preparation and the unique three-dimensional organization of the TTF salt of the latter paramagnetic cluster anion. The structural description of the title compound demonstrates that this is in fact a molecular rock salt structure in which all the T_d sites are accessible and selectively occupied. Thus, channels are created that incorporate acetonitrile molecules. X-ray diffuse scattering experiments providing evidence and estimation of the movements of the neutral molecules in the channels are reported. Furthermore, our structural work, supplemented by single-crystal ESR data, characterizes an unusual magnetic interaction between the triplet state of the $(TTF^+)_2$ dimers and the paramagnetic niobium cluster halide.

Experimental Section

Preparation of $(TTF)_2(Nb_6Cl_{18})(Et_4N)(CH_3CN)$. The solvents were dried and degassed prior to utilization, and the electrochemical cells degassed with argon. Well-faceted, black shiny single crystals of the title compound were grown at a platinum wire anode under constant current electrolysis (J = 1.6 μA cm^{-2}, 19 days) of 30 cm^3 of a CH_3CN:CH_2Cl_2 (5:1) solution (purified over activated neutral alumina) containing the donor (TTF, 14 mg, 0.06 mmol, Fluka, purified by sublimation) and $(Et_4N)_3Nb_6Cl_{18}$ (0.10 g, 0.06 mmol). The latter was prepared as described previously.[6,7] The composition has been determined by resolution of the crystal structure.

Crystal Data. $Nb_6Cl_{18}S_8N_2C_{22}H_{31}$, FW = 1775.61; tetragonal, a = 17.929 (6), c = 15.798 (3) Å, V = 5079.0 Å^3 (determined by

(1) (a) Wells, A. F. *Structural Inorganic Chemistry*; Clarendon Press: Oxford, 1986. (b) Hyde, B. G.; Andersson, S. *Inorganic Crystal Structures*; John Wiley: New York, 1989.

(2) (a) Burdett, J. K. *Chem. Rev.* **1988**, *88*, 1. (b) von Schnering, H. G.; Hönle, W. *Ibid.* **1988**, *88*, 243. (c) Fagan, P. J.; Ward, M. D.; Calabrese, J. C. *J. Am. Chem. Soc.* **1989**, *111*, 1698. Ward, M. D.; Fagan, P. J.; Calabrese, J. C.; Johnson, D. C. *Ibid.* **1989**, *111*, 1719.

(3) (a) Batail, P.; Ouahab, L. *Mol. Cryst. Liq. Cryst.* **1985**, *125*, 205. (b) Ouahab, L.; Batail, P.; Perrin, C.; Garrigou-Lagrange, C. *Mater. Res. Bull.* **1986**, *21*, 1223.

(4) Batail, P.; Ouahab, L.; Penicaud, A.; Lenoir, C.; Perrin, A. C. R. *Hebd. Seances Acad. Sci., Paris.* **1987**, *304 Sér. II*, 1111. Renault A.; Pouget J. P.; Parkin, S. S. P.; Torrance, J. B.; Ouahab, L.; Batail, P. *Mol. Cryst. Liq. Cryst.* **1988**, *161*, 329. Penicaud, A.; Lenoir, C.; Batail, P.; Coulon, C.; Perrin, A. *Synth. Met.* **1989**, *32*, 25.

(5) (a) Penicaud, A.; Batail, P.; Perrin, C.; Coulon, C.; Parkin, S. S. P.; Torrance, J. B. *J. Chem. Soc., Chem. Commun.* **1987**, 330. (b) Penicaud, A.; Batail, P.; Tomić, S.; Jerome, D.; Coulon C. *Synth. Met.* **1988**, *27*, B103. (c) Penicaud, A.; Batail, P.; Coulon C.; Canadell, E.; Perrin, C. *Chem. Mater.*, following paper in this issue.

(6) Koknat, F. W.; Parson, J. A.; Vongvusharintra, A. *Inorg. Chem.* **1974**, *13*, 7.

(7) Mackay, R. A.; Schneider, R. F. *Inorg. Chem.* **1967**, *6*, 549.

0897-4756/90/2802-0117$02.50/0

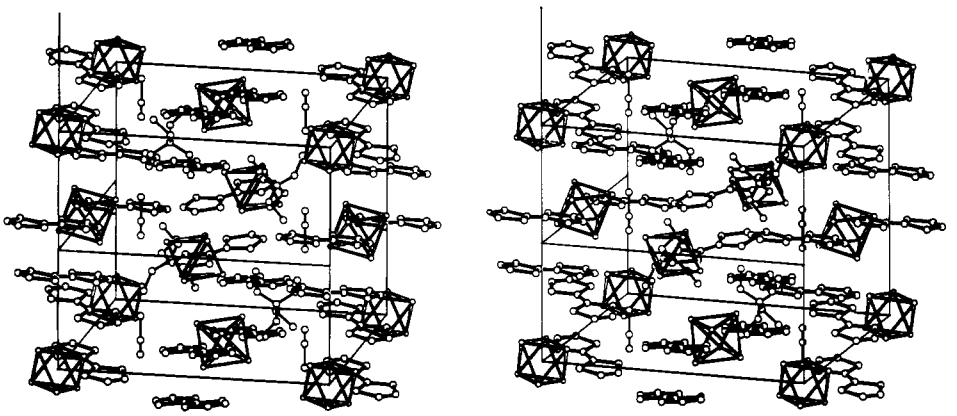

Figure 1. Stereographic view of the unit-cell content shifted of $c/2$; the a axis runs horizontally and the c axis vertically. The chlorine atoms coordinating the Nb_6 cluster core (Figure 5) and hydrogen atoms have been omitted for clarity.

Table I. Non-Hydrogen Atomic Coordinates ($\times 10^4$) and Equivalent Isotropic Thermal Parameters

atom	x	y	z	E_{eq}/Å^2
Nb(1)	-1001.1 (2)	4828.3 (2)	-672.4 (2)	0.762 (7)
Nb(2)	593.9 (2)	4406	-940.2 (3)	0.730 (6)
Cl(1)	-954.8 (7)	5955	-1529.3 (8)	1.16 (2)
Cl(2)	-1351.8 (6)	3648	0	1.13 (2)
Cl(3)	470.1 (7)	3166.4 (6)	-311.3 (6)	1.20 (2)
Cl(4)	-472.0 (6)	4120.6 (6)	-1850.2 (6)	1.08 (2)
Cl(5)	-2201.1 (7)	4653.4 (7)	-1483.8 (6)	1.42 (2)
Cl(6)	1312.4 (7)	3682	-2038.7 (9)	1.46 (2)
S(1)	5094.2 (7)	1055.0 (7)	5954.5 (6)	1.41 (2)
S(2)	5206.9 (7)	-1347.8 (7)	6321.9 (7)	1.54 (2)
C(1)	4876 (3)	124	6038 (4)	1.37 (8)
C(2)	5419 (3)	-419	6205 (4)	1.13 (8)
C(3)	4182 (3)	1340 (3)	5802 (2)	1.7 (1)
C(4)	6117 (3)	-1642 (3)	6448 (2)	1.7 (1)
N(1)	-2500	2500	-2500	1.1 (1)
C(5)	-3184 (3)	2346 (3)	-1954 (3)	1.3 (1)
C(6)	-3347 (3)	2948 (3)	-1304 (3)	2.0 (1)
N(2)	2500	2500	-4966 (8)	4.9 (2)
C(7)	2500	2500	-4300 (10)	4.2 (3)
C(8)	2500	2500	-3353 (8)	5.4 (2)

least-squares refinement of the angular coordinates of 24, reflections with θ varying from 15 to 23°, temperature = 140 K; Mo Kα radiation, λ = 0.71069 Å; space group $P4_2/ncm$ (origin at center 2/m); D_m = 2.27 g cm^{-3} (flotation method), Z = 4, D_x (295 K) = 2.26 g cm^{-3}; black polyhedron, 0.09 × 0.15 × 0.18 mm^3, μ = 26 cm^{-1}.

Data Collection and Processing.[8] Enraf-Nonius CAD4-F diffractometer equipped with a cold nitrogen stream cryostat, $\omega/2\theta$ mode with ω scan width 1 + 0.35 tan θ, graphite-monochromated Mo Kα radiation; 5510 reflections measured ($1 \le \theta \le 26°$, $+h,k,l$), 2941 unique reflections [merging R = 4.8% after absorption correction[9] based on ψ scans (minimum relative transmission = 79%)] giving 1681 reflections with $I > 3\sigma(I)$. Intensity controls every hour of measuring time showed maximum variation of 1.6%.

Structure Analysis and Refinement. The structure was solved by a combination of direct methods and Fourier techniques and refined (full-matrix least-squares) anisotropically with hydrogen atoms included in scale factor calculations at ideal positions and not refined. The weighting scheme used was $1/w = (\sigma^2(I) + (0.02F_o^2)^2)/4F_o^2$, with $\sigma(I)$ from counting statistics. Final R and R_w values are 0.023 and 0.027, the goodness of fit is 1.001. Scattering factors are from International Tables for X-ray Crystallography, all computer programs are from the Enraf-Nonius Structure Determination Package.[8] The final positional parameters are given Table I.

X-ray Diffusion Photographs. Graphite-monochromated Cu Kα radiation was used with fixed film, fixed-crystal, vacuum chamber, from room temperature to 15 K, following routine procedures developed in this laboratory.[10]

Physical Measurements. ESR spectra were recorded on a Varian X-band spectrometer (frequency = 9.3 GHz) from room to liquid helium temperature. Conductivity was checked on a single crystal by using the standard four-probe dc technique. Mass spectrometry was performed at the Centre Régional de Mesures Physiques de l'Ouest, University of Rennes-I on a Varian MAT 311 spectrometer under 10^{-6} mmHg.

Table II. Interatomic Distances (angstroms) within the Cluster Unit[a]

atom	atom	dist	atom	atom	dist
Nb(1)	Nb(1a)	2.9885 (9)	Nb(1)	Cl(3)	2.442 (1)
Nb(1)	Nb(1b)	2.973 (1)	Nb(1)	Cl(4)	2.443 (1)
Nb(1)	Nb(2)	2.9879 (7)	Nb(1)	Cl(5)	2.524 (1)
Nb(1)	Nb(2a)	2.9836 (6)	Nb(2)	Cl(3)	2.444 (1)
Nb(1)	Cl(1)	2.433 (1)	Nb(2)	Cl(4)	2.445 (1)
Nb(1)	Cl(2)	2.449 (1)	Nb(2)	Cl(6)	2.515 (1)

[a] Symmetry codes: (a) ($y - {}^1/_2$, ${}^1/_2 + x$, $-z$); (b) (${}^1/_2 - y$, ${}^1/_2 - x$, z). Cl_b: Cl(1), Cl(2), Cl(3), Cl(4). Cl_t: Cl(5), Cl(6).

Results and Discussion

Crystal and Molecular Structure. A stereoscopic view of the unit cell is shown in Figure 1. Averaged bond distances for the TTF molecule are given in Table III; the atom numbering and bond distances for the cluster are given in Figure 5 and Table II, respectively. The centrosymmetrical $(TTF^+)_2$ dimers and cluster anions are located at the 4d sites (0, 0, 0) and 4c sites (0, 0, ${}^1/_2$), respectively, and the tetraethylammonium cations Et_4N^+ at the 4b sites (${}^3/_4$, ${}^1/_4$, ${}^3/_4$). Therefore, the basic structural framework (Figure 1) is a face-centered pseudocubic (c/a = 0.89) array of cluster anions in which discrete $(TTF^+)_2$ dimers fill in all the six-coordinated sites (centers of the translated unit cell and of the vertices, Figure 1). This arrangement is that of a NaCl-type structure. Since additional cations are needed to reach neutrality, tetraethylammonium cations (Et_4N^+) fill half of the four-coordinated sites (Figure 1). However, due to the pronounced asymmetry of $(TTF^+)_2$ when compared to the essentially spherical ions Et_4N^+ and $Nb_6Cl_{18}^{3-}$, the four filled four-coordinated sites are not evenly distributed in the tetrahedral pattern 1 as in the zinc blende type structure. Rather, all the tetrahedral sites are either successively filled or empty (pattern **2**) in the direction parallel to the c axis of the quadratic unit cell. Therefore, the remaining four ion-free tetrahedral sites generate infinite parallel channels incorporating four acetonitrile molecules (Figure 2). The carbon and nitrogen

(8) Frenz, B. A. *Computing in Crystallography*; Delft University Press: Delft, The Netherlands, 1978.
(9) North, A. C. T.; Phillips, D. C.; Mathews, F. S. *Acta Crystallogr., Sect. A.* **1968**, *24*, 351.
(10) Comes, R.; Lambert, M.; Guinier, A. *Acta Crystallogr.* **1970**, *26*, 244.

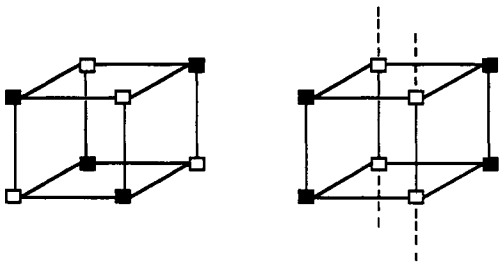

1 2

atoms of the solvent molecule were located unambiguously on a difference Fourier synthesis, and their positional and anisotropic thermal parameters were properly refined. However, the comparatively large values for both the isotropic thermal parameters and the root-mean-square amplitudes of the thermal vibrations for atoms N(2), C(7), and C(8) account for a significant amount of motion of the solvent molecule at 140 K (vide infra).

The bond distances in the TTF molecule are compared in Table III with those observed for other TTF salts with a variety of degrees of charge transfer. Clearly, in this compound the donor molecule is fully oxidized. The discrete divalent cations $(TTF^+)_2$ exhibit (Figure 3) a slipped bond-over-ring type of overlap with a lateral shift along the in-plane molecular axis (δ = 1.47 Å at 295 K) and a 3.47-Å (295 K) interplanar separation (Table IV), typical of those observed for the uniform donor stack in TTF–TCNQ.[11] This contrasts with the geometry reported[12] for most of the TTF salts with fully oxidized isolated dimers in which an eclipsed configuration and a shorter (3.40 Å) interplanar separation (Table IV) indicate a stronger intradimer transfer integral. The present dimer configuration (Figure 3) is also very similar to that observed for the 2:1 radical cation salts of tetramethyltetrathiafulvalene (commonly abbreviated TMTTF), $(TMTTF)_2X$.[13] Therefore, the charge-transfer integral has the same order of magnitude, i.e., t = 0.14 eV.[14] Indeed, a calculation[14] using our structural data gives t = 0.12 eV with the 15% difference exactly accounted for by the electron-donating effect of the methyl substituents. This further demonstrates that the intradimer overlap in the discrete $(TTF^+)_2$ dimers is similar to that observed in a conducting chain.

Inside the octahedral void of niobium clusters depicted in Figure 4, the organic dimer is surrounded by numerous chlorine atoms. One sulfur–chlorine contact is significantly shorter (3.268 (2) Å) than the sum of the van der Waals radii (3.65 Å)[15] and comparable to similar close contacts in other charge-transfer salts with metal halide anions, for example, $(TMTTF)_5(Nb_6Cl_{18})(CH_2Cl_2)_{0.5}$[3.330 (3) Å][5] and $(TTF)_3SnCl_6$[3.367 (2) Å].[16]

The average $\angle Cl_bNbCl_b$ (165.3(2)°) and $\angle NbCl_bNb$ (75.29 (6)°) angles as well as the average Nb–Cl_t distance (2.518 (4) Å; Cl_b and Cl_t are bridging and terminal chlorine atoms,

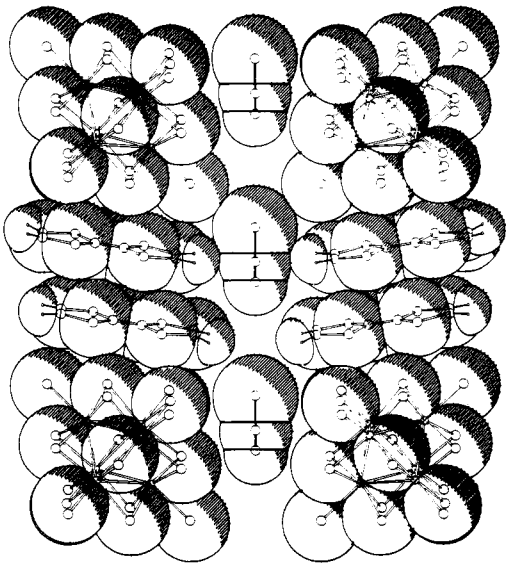

Figure 2. Projection onto (c, a + b), showing the channels along c with the acetonitrile molecules.

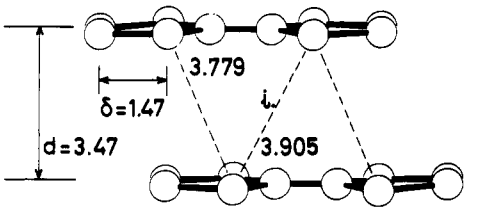

Figure 3. Intradimer interaction at 295 K (distances in angstroms).

respectively) are as expected for a 15-electron $Nb_6Cl_{12}^{3+}$ cluster core (Figure 5).[17] The average Nb–Nb bond length of 2.984 (5) Å appear to be larger than that calculated (2.967 (17) Å) for the same cluster anion in $(Me_4N)_3Nb_6Cl_{18}$,[18] although the large dispersion of the bond distances in the latter salt precludes any significant conclusion. On the other hand, the corresponding average bond length of 2.956 (5) Å in $LuNb_6Cl_{18}$[19] is significantly shorter. Therefore, we conclude that the Nb_6 octahedron is slightly expanded in the present compound. This is a distinctive common feature of the organic charge-transfer salts prepared so far[5] with this molecular cluster anion.

Analysis of the Molecular Movements in the Channels. Photographs taken at 300 and 15 K (Figures 6a,b) with the reciprocal c^* axis horizontal show the presence of scattered intensity localized off the Bragg spots. These diffuse lines correspond to the intersection with the Ewald sphere of a family of equidistant diffuse planes normal to the reciprocal c^* axis. These planes are characteristic of one-dimensional disorder along the channels axis c.[20] Such diffuse planes are displayed for example in charge-transfer salts such as $DiPS\Phi_4(I_3)_{0.76}$[21] or $Hg_{3-\delta}AsF_6$,[22] where they were ascribed to disorder along iodide and mercury chains, respectively. The intensity of the diffuse planes decreases with temperature, implying

(11) Kistenmacher, T. J.; Phillips, T. E.; Cowan, D. O. *Acta Crystallogr., Sect. B.* **1974**, *30*, 763.
(12) See for example, ref 3b and the following: (a) Teitelbaum, R. C.; Marks, T. J.; Johnson, C. K. *J. Am. Chem. Soc.* **1980**, *102*, 2986. (b) Yakushi, K.; Nishimura, S.; Sugano, T.; Kuroda, H. *Acta Crystallogr. Sect. B* **1980**, *36*, 358.
(13) Liautard, B.; Peytavin, S.; Brun, G.; Maurin, M. *J. Phys. (Orsay)* **1982**, *43*, 1453.
(14) Ducasse, L.; Abderraba, A.; Hoarau, J.; Pesquer, M.; Gallois, B.; Gaultier, J. *J. Phys. C: Solid State Phys.* **1986**, *19*, 3805.
(15) Pauling, L. *The Nature of the Chemical Bond*; Cornell University Press: Ithaca, NY, 1960.
(16) Kondo, K.; Matsubayashi, G.; Tanaka, T.; Yoshioka, H.; Nakatsu, K. *J. Chem. Soc., Dalton Trans.* **1984**, 379.
(17) A detailed discussion of the molecular structure of the $Nb_6Cl_{12}^{n+}$ cluster core is to be found in ref 18. See also Table VII in ref 5c.
(18) Koknat, F. W.; McCarley, R. E. *Inorg. Chem.* **1974**, *13*, 295.
(19) Ihmaine, S.; Perrin, C.; Peña, O.; Sergent, M. *J. Less-Common Met.* **1988**, *137*, 323.
(20) Guinier, A. *X-ray Diffraction in Crystals, Imperfect Crystals and Amorphous Bodies*; W. H. Freeman and Co.: San Francisco, 1963.
(21) Albouy, P. A.; Pouget, J. P.; Strzelecka, H. *Phys. Rev. B* **1987**, *35*, 173.
(22) Pouget, J. P.; Shirane, G.; Hastings, J. M.; Heeger, A. J.; Miro, N. D.; McDiarmid, A. G. *Phys. Rev. B* **1978**, *18*, 3645.

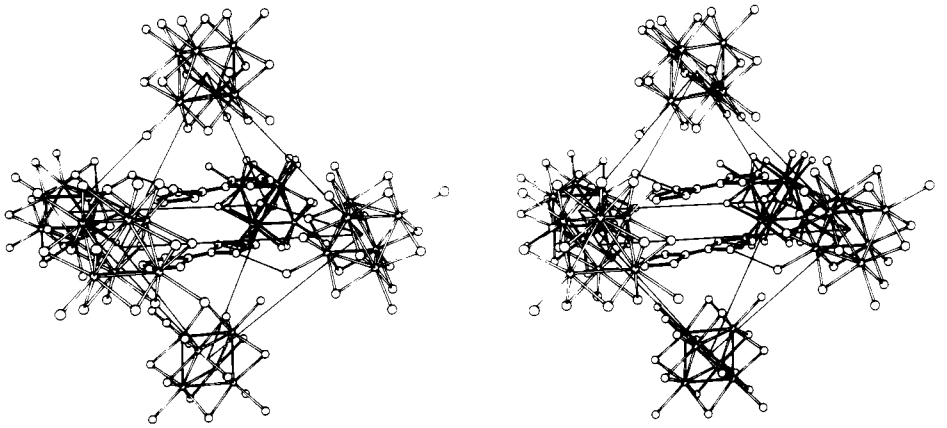

Figure 4. Stereoscopic view of the pseudooctahedral arrangement of $Nb_6Cl_{18}^{3-}$ anions surrounding the divalent dimers $(TTF^+)_2$.

Table III. Bond Distances (angstroms) in the TTF Molecule Averaged in D_{2h} Symmetry in $(TTF)_2(Et_4N)(Nb_6Cl_{18})(CH_3CN)$ and in Selected TTF Salts from the Literature

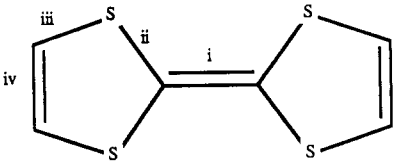

compd	charge per TTF	dist i	dist ii	dist iii	dist iv
TTF[a]	0.0	1.349 (3)	1.757 (2)	1.726 (4)	1.314 (3)
TTF-TCNQ[b]	0.59	1.369 (4)	1.743 (4)	1.736 (5)	1.323 (4)
$TTF{\cdot}I_3$[c]	1.0	1.382 (7)	1.719 (8)	1.728 (11)	1.322 (11)
$TTF\text{-}ClO_4$[d]	1.0	1.403	1.713	1.725	1.306
$(TTF)_2(Et_4N)(Nb_6Cl_{18})(CH_3CN)$	1.0	1.400 (7)	1.719 (6)	1.729 (6)	1.32 (1)

[a] Cooper, W. F.; Kenney, N. C.; Edmonds, J. C.; Nagel, A.; Wudl, F.; Coppens, P. *J. Chem. Soc., Chem. Commun.* **1971**, 889. [b] Kistenmacher, T. J.; Philips, T. E.; Cowan, D. O. *Acta Crystallogr., Sect. B* **1974**, *30*, 763. [c] Teitelbaum, R. C.; Marks, T. J.; Johnson, C. K. *J. Am. Chem. Soc.* **1980**, *102*, 2986. [d] Yakushi, K.; Nishimura, S.; Sugano, T.; Kuroda, H. *Acta Crystallogr., Sect. B.* **1980**, *36*, 358.

Table IV. Interplanar Distance *d* (angstroms) and Lateral Shift δ (angstroms) (See Figure 3 and Text) for TTF Dimers in $(TTF)_2(Et_4N)(Nb_6Cl_{18})(CH_3CN)$ and in Selected TTF Salts from the Literature

compound	donor unit	interplanar dist *d*	lateral shift δ
$(TTF)_2(Et_4N)$-$(Nb_6Cl_{18})(CH_3CN)$	dimer	3.47[a] (3.39[b])	1.47[a] (1.41[b])
TTF-TCNQ[c]	stack	3.47	1.60
$TTF{\cdot}I_3$[d]	dimer	3.40	0.25
$TTF\text{-}ClO_4$[e]	dimer	3.41	≈0
$(TTF)(SnMe_2Cl_3)$[f]	dimer		0.62

[a] Reference 5b. [b] At 140 K. [c] Reference b of Table III. [d] Reference c of Table III. [e] Reference d of Table III. [f] Matsubayashi, G.; Ueyama, K.; Tanaka, T. *J. Chem. Soc., Dalton Trans.* **1985**, 465.

that the one-dimensional disorder is dynamic in nature.[20] It reaches a maximum every fourth plane in each reciprocal unit cell at room temperature (Figure 6a) as well as at 15 K (Figure 6b). This provides a crude estimate[10] of the amplitude of the movements of ca. 3–4 Å. In addition, from the large values of the thermal parameters for atoms N(2), C(7), and C(8) and the pronounced anisotropy of the central carbon atom C(7), it can be inferred that most of the observed disorder is related to significant movements of the acetonitrile molecules along their long axis in the channels. The magnitude of the thermal parameters of N(2), C(7), and C(8) gives another crude estimate of the 1-D movements of about 1 Å. A precise determination of this value would require a much more extensive study, and we shall not go further than stating that the amplitude of

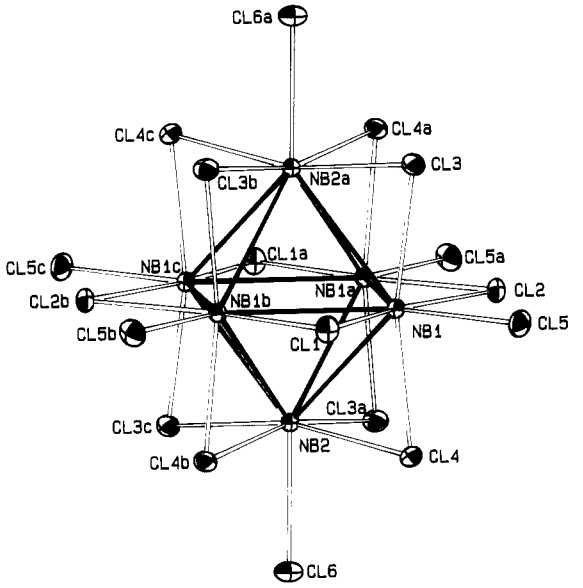

Figure 5. Atom numbering in the cluster unit. Symmetry codes: (a) $(y - {}^1/_2, {}^1/_2 + x, -z)$; (b) $({}^1/_2 - y, {}^1/_2 - x, z)$; (c) $(-x, 1 - y, -z)$.

the movements of the acetonitrile molecules in the channels is on the order of an angstrom. Note also that mass spectrometry experiments reveal the concomitant emergence at 155 °C of molecular ions at m/z = 41 (CH_3CN^+), 102 (TTF^{2+}), and 204 (TTF^+), which tends to suggest that the acetonitrile molecules are necessary to the stability of the structure.

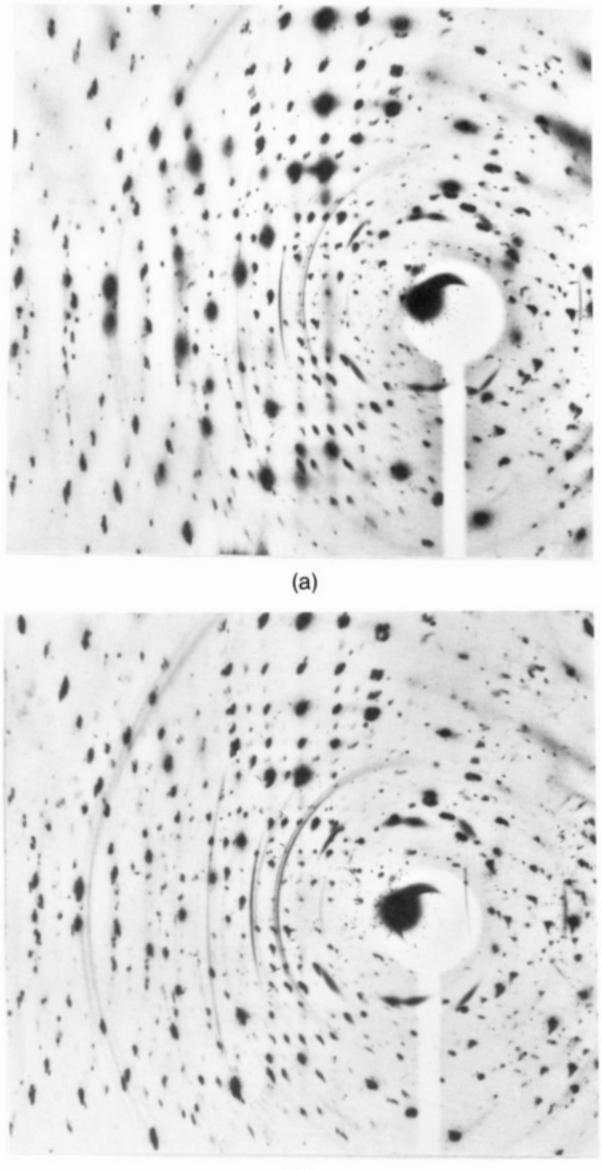

Figure 6. Fixed-film, fixed-crystal X-ray photographs with the reciprocal c^* axis horizontal: (a) T = 295 K; (b) T = 15 K.

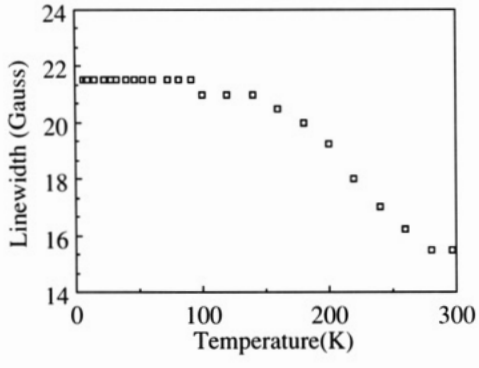

Figure 7. Temperature dependence of the ESR line width.

ESR Results. A single line with a Lorentzian shape and isotropic characteristics (g = 1.9674 and peak-to-peak line width ΔH = 15 G at room temperature) is observed by electron spin resonance. This line remains unique and isotropic upon cooling of the sample down to 5 K. The line width is slighlty temperature dependent (Figure 7) and is significantly smaller than the value determined (115 G) for a powder sample of the ammonium salt $(Et_4N)_3Nb_6Cl_{18}$.

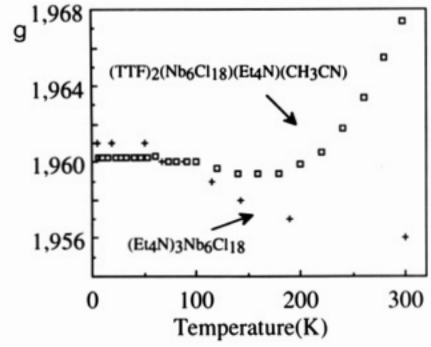

Figure 8. Temperature dependence of the g factor for $(TTF)_2(Et_4N)(Nb_6Cl_{18})(CH_3CN)$ and $(Et_4N)_3(Nb_6Cl_{18})$.

The temperature dependence of the g value is plotted and compared in Figure 8 with that of the cluster spin in $(Et_4N)_3Nb_6Cl_{18}$ as a reference. There is a large offset between the g value for $(TTF)_2(Nb_6Cl_{18})(Et_4N)(CH_3CN)$ and that of the ammonium salt at room temperature. This offset gradually decreases with temperature, and the g values finally merge at 120 K downward.

At the onset of the discussion of the ESR data, it should be pointed out that, besides the localized cluster spin, there is no other spin in the compound since the fully oxidized $(TTF^+)_2$ dimer is expected to present a diamagnetic ground state.[23] However, due to the observed offset of the g values, the room-temperature resonance cannot be assigned to that of the localized cluster spin alone. Therefore, we suggest that the triplet state of the dimer is partially populated at high temperature. In the absence of interactions between the two spin systems, the ESR spectra would display two different resonances. Instead, coupling between the two systems causes the two resonances to merge into one line. At low temperature (T < 120 K) the dimer is in the diamagnetic ground state, and the g value for the compound is that of the cluster spin. At higher temperatures, the triplet state of the dimer becomes increasingly occupied and, due to the interaction, the g value increases as the proportion of unpaired organic spin toward the average value for $TTF^{\bullet+}$ (g_c = 2.008).[24] The g value of the resulting single line is the susceptibility-weighted sum of the individual g values:[25]

$$g_{obs} = \alpha_a g_a + \alpha_c g_c \quad (1)$$

where α_a and α_c are the fractional spin susceptibilities:

$$\alpha_a = \chi_a/(\chi_a + \chi_c)$$

$$\alpha_c = \chi_c/(\chi_a + \chi_c)$$

and χ_a and χ_c are the individual systems susceptibilities for the anion and the dimeric cation respectively. From eq 1, α_a and α_c read

$$\alpha_a = (g_{obs} - g_c)/(g_a - g_c) \quad (2)$$

$$\alpha_c = 1 - \alpha_a$$

(23) (a) Jacobs, I. S.; Bray, J. W.; Hart, H. R.; Interrante, L. V.; Kasper, J. S.; Watkins, G. D.; Prober, D. E.; Bonner, J. C. *Phys. Rev. B: Solid State* **1976**, *14*, 3036. (b) Bray, J. W.; Interrante, L. V.; Jacobs, I. S.; Bonner, J. C. In *Extended Linear Chain Compounds*; Miller, J. S., Ed.; Plenum: New York, 1983; Vol. 3, p 353.

(24) Wudl, F.; Smith, G. M.; Hufnagel, E. J. *J. Chem. Soc., Chem. Commun.* **1970**, 1453.

(25) Tomkiewicz, Y. *The Physics and Chemistry of Low Dimensional Solids*; D. Reidel: Boston, 1980. Ogawa, M. Y.; Martinsen, J.; Palmer, S. M.; Stanton, J. L.; Tanaka, J.; Greene, R. L.; Hoffman, B. M.; Ibers, J. A. *J. Am. Chem. Soc.* **1987**, *109*, 1115. Tomkiewicz, Y.; Taranko, A. R.; Torrance, J. B. *Phys. Rev. Lett.* **1976**, *36*, 751.

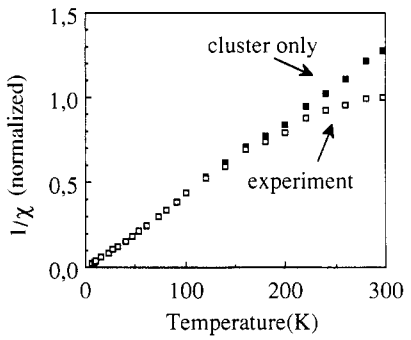

Figure 9. Temperature dependence of the normalized, reciprocal spin susceptibilities. The cluster-only data were extrapolated from the experiment as indicated in the text.

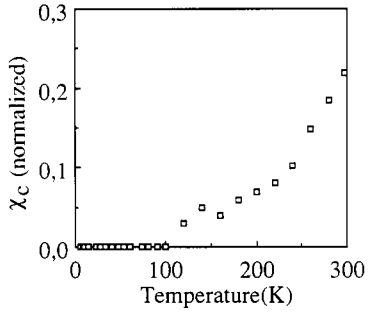

Figure 10. Temperature dependence of the normalized spin susceptibility χ_c for $(TTF^+)_2$ calculated from the ESR experiment (see text).

which, in turn, allow the calculation of the individual spin susceptibilities χ_a and χ_c:

$$\chi_a = \alpha_a \chi_{obs} \qquad (3)$$

$$\chi_c = \alpha_c \chi_{obs}$$

where $\chi_{obs} = \chi_a + \chi_c$ is the observed spin susceptibility.

The temperature dependences of the reciprocal normalized spin susceptibilities χ_{obs}^{-1} and χ_a^{-1} are given Figure 9, and that of the normalized susceptibility χ_c for $(TTF^+)_2$ is shown in Figure 10. The observed normalized susceptibility for the compound follows a Curie law at low temperature. The deviation from the linear behavior of the reciprocal susceptibility at high temperature indicates the onset of the contribution of the organic dimer triplet state to the compound susceptibility. The cluster anion susceptibility itself obtained from the present g decomposition technique follows a Curie law up to room temperature as expected for a system of noninteracting localized spins. The susceptibility for $(TTF^+)_2$ (Figure 10) shows up at 120 K and increases exponentially with temperature.

The activated spin susceptibility χ_c for the organic dimer can be expressed as

$$\chi_c = C/T \exp(-\Delta/k_B T) \qquad \text{for } \Delta \gg k_B T \qquad (4)$$

where Δ represents the singlet–triplet energy gap. The expected linear relationship

$$\ln(\chi_c T) = -(\Delta/k_B)/T + \ln C \qquad (5)$$

is indeed verified (Figure 11) within experimental accuracy.[26] One then estimates a singlet–triplet energy gap Δ of ca. 0.07–0.10 eV (Δ/k_B = 850–1100 K).

The magnitude of this magnetic gap can be understood by simple arguments. Since the dimers are quasiisolated

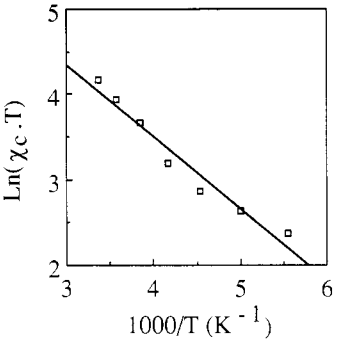

Figure 11. Linear fit to $\ln(\chi_c T) = -(\Delta/k_B)/T + \ln C$ for the dimer-only spin susceptibility.

as indicated by the crystal structure analysis, a model of noninteracting dimers is appropriate to understand the organic component of the magnetic susceptibility.

The eigenvalues of a divalent dimer are well-known, considering a Hubbard Hamiltonian. Two parameters are to be introduced: t, the intradimer transfer integral, and U_{eff}, the effective on-site repulsion for the two electrons. In the present case, we simply have

$$U_{eff} = U - V_1$$

where U is the bare on-site repulsion and V_1 the repulsion when the electrons are on neighboring sites. U_{eff} has been estimated[27] for various organic compounds and is typically ca. 0.7–1.0 eV.

Based on these two parameters, the magnetic gap reads[28]

$$\Delta = \tfrac{1}{2}(U_{eff}^2 + 16t^2)^{1/2} - U_{eff}/2$$

With U_{eff} = 0.7 eV and t = 0.12 eV (vide infra), one calculates Δ = 0.074 eV, in fair agreement with our estimation of the magnetic gap.

Conclusion

The compound $(TTF^+)_2[(Nb_6Cl_{18})^{3-}][(C_2H_5)_4N^+][CH_3CN]$ has been prepared by electrocrystallization. Its structure presents a unique molecular rock salt framework of cluster anions and discrete $(TTF^+)_2$ dimers with half of the tetrahedral interstices selectively occupied by tetraethylammonium cations. Infinite channels incorporating acetonitrile molecules are created, and they connect the other four tetrahedral sites. The amplitude of the movements of the solvent molecules along the channel axis is on the order of an angstrom. In this insulating compound, the intradimer interaction is considerably less than expected for isolated divalent $(TTF^+)_2$. In fact, the fully oxidized dimer configuration and the calculated intradimer transfer integral are similar to those usually observed in mixed-valence conducting chains. These structural features are supplemented by the observation of a single ESR line that cannot be assigned to that of the localized cluster spin only for temperatures above ca. 120 K. The structure analysis and the ESR studies both suggest that the triplet state of the dimer is partially populated at high temperature, and it interacts with the localized niobium cluster spin. A simple model based on the Hubbard Hamiltonian for noninteracting dimers gives a magnetic gap of 0.07 eV, which agrees with the experimental value of 0.07–0.10 eV deduced from an analysis of the spin susceptibility. Besides, the inorganic part of the compound susceptibility follows a Curie law up to room temperature, thus indicating that the niobium cluster spins do not interact with

(26) Note that only data points for temperatures over 170 K ($1000/T < 6$) have been included in the linear fit. At lower temperatures the dimer susceptibility is extremely low and of the order of the error bar.

(27) Mazumdar, S.; Dixit, S. N. *Phys. Rev. B* **1986**, *34*, 3683.
(28) Harris, A. B.; Lange, R. V. *Phys. Rev.* **1967**, *157*, 295.

each other. Altogether, by use of these organic–inorganic building blocks, a specific and rational crystalline arrangement is achieved. We believe that this could be the base for further substitution at particular molecular ion sites in order to modify such unique properties of this hybrid salt as the peculiar slight expansion of the metal–metal bond lengths in the Nb_6 cluster core or the organic dimer–metal cluster magnetic interaction.

Acknowledgment. We thank the C.N.R.S. (ATP-PIRMAT Chimie Douce) for their support, Dr. L. Ducasse of Université de Bordeaux I for the intradimer transfer integral calculation, and Dr. P. Guénot, Université de Rennes I, for the mass spectrometry experiments.

Registry No. TTF, 31366-25-3; $(TTF)_2(Nb_6Cl_{18})(Et_4N)(CH_3CN)$, 124854-80-4; $(Et_4N)_3Nb_6Cl_{18}$, 12128-45-9.

Supplementary Material Available: Tables of atomic coordinates (including hydrogen atoms), anisotropic thermal parameters, and all bond lengths and angles (4 pages); observed and calculated structure factors (5 pages). Ordering information is given on any current masthead page.

Novel Redox Properties of the Paramagnetic Hexanuclear Niobium Cluster Halide $Nb_6Cl_{18}^{3-}$ and the Preparation, Structures, and Conducting and Magnetic Properties of Its One-Dimensional Mixed-Valence Tetramethyltetra(selena and thia)fulvalenium Salts: [TMTSF and TMTTF]$_5$[Nb_6Cl_{18}]·$(CH_2Cl_2)_{0.5}$

Alain Pénicaud and Patrick Batail*

Laboratoire de Physique des Solides Associé au CNRS, Université de Paris-Sud, 91405 Orsay, France

Claude Coulon

Centre de Recherche Paul Pascal, CNRS, Domaine Universitaire de Bordeaux I, 33405 Talence, France

Enric Canadell

Laboratoire de Chimie Théorique Associé au CNRS, Université de Paris-Sud, 91405 Orsay, France

Christiane Perrin

Laboratoire de Chimie Minérale B Associé au CNRS, Université de Rennes I, 35042 Rennes, France

Received July 31, 1989

A cyclic voltammetry study in acetonitrile of $[(C_2H_5)_4N]_3Nb_6Cl_{18}$ is presented that gives the first evidence for the existence at 1.72 V vs SCE of the 13-electron cluster core $Nb_6Cl_{12}^{5+}$, a novel powerful inorganic oxidant. The title compounds have been prepared by electrocrystallization and characterized by single-crystal X-ray diffraction, ESR, and magnetic susceptibility and transport experiments. $[(D)_4^{3+}(D^0)]Nb_6Cl_{18}^{3-}(CH_2Cl_2)_{0.5}$ [D = 2,3,6,7-tetramethyl-1,4,5,8-selena- and thiafulvalene (TMTSF and TMTTF) in **1** and **2**, respectively] are semiconducting ($\sigma_{300\,K}$ = 0.5 Ω^{-1} cm^{-1} for **1**; activation energies of 0.16 and 0.20 eV for **1** and **2**, respectively) and the triclinic (space group $P\bar{1}$) unit-cell parameters are a = 13.176 (5), b = 13.847 (7), c = 14.581 (9) Å, α = 113.79 (3), β = 96.47 (3), γ = 99.94 (3)°, V = 2348.1 (2) Å^3 for **1** and a = 12.933 (7), b = 13.669 (8), c = 14.334 (11) Å, α = 114.40 (3), β = 96.97 (4), γ = 99.21 (4)°, V = 2227.8 (3) Å^3 for **2**. Both salts are isostructural and present stacks of the organic radical cations with one-dimensional electronic properties. The electronic structure of these salts has been studied by means of tight-binding band structure calculations. A unique magnetic interaction between the organic spins and the localized inorganic cluster spins is presented and discussed.

Introduction

Since the pioneering work of Siedle,[1] the chemistry of tetrathiafulvalene (TTF) and its substituted derivatives with transition-metal halides has been expanding rapidly with the aim of combining highly anisotropic electrical properties and extended TTF–metal interactions. Many different types of materials have been prepared based on discrete and polymeric inorganic metal halides with a variety of coordination geometries.[2] In addition, oxidizing organometallic halides have recently been engaged in

(1) (a) Siedle, A. R.; Candela, G. A.; Finnegan, T. F.; Van Duyne, R. P.; Cape, T.; Kokoszka, G. F.; Woyciesjes, P. M.; Hashmall, J. A.; Glick, M.; Isley, W. *Ann. N.Y. Acad. Sci.* **1978**, *313*, 377. (b) Siedle, A. R *Extended Linear Chain Compounds*; Miller, J. S., Ed.; Plenum Press: New York, 1982; p 469.

(2) For a recent survey, see the proceedings of the International Conference on Science and Technology of Synthetic Metals, Santa Fe; *Synth. Met.* **1988**, *27*, nos. 1–4.

0897-4756/90/2802-0123$02.50/0